Journal of Applied Electrochemistry **32**: 1247–1255, 2002.

Electrochemical nucleation and growth of copper on chromium-plated electrodes

S-B. KIM, K-T. KIM, C-J. PARK and H-S. KWON*
Department of Material Science and Engineering, Korea Advanced Institute of Science & Technology, 373-1 Ku SongDong, YuSongKu, TaeJon, 305-701 Korea
*(*author for correspondence, e-mail: hskwon@mail.kaist.ac.kr)*

Received 2 January 2001; accepted in revised form 24 July 2002

Key words: copper, chromium, electrodeposition, electrochemical nucleation

Abstract

Nucleation and growth of copper electrodeposited on chromium plated electrodes in copper sulfate electrolytes were examined, focusing on the influence of prior Cr plating conditions on the nucleation density and growth kinetics of the copper electrodeposits. The Cr-plated electrodes were made by electrodeposition of Cr on copper sheets for 2 to 60 s at 0.1 A cm^{-2} in CrO_3 350 g L^{-1} + H_2SO_4 3.5 g L^{-1}. Copper was then electrodeposited onto the Cr-plated electrode under potentiostatic conditions. Copper initially nucleated and grew according to a three-dimensional diffusion controlled progressive nucleation process, and later according to an instantaneous nucleation process. The period during which copper nucleation is controlled by the diffusion controlled progressive nucleation process decreases with increasing Cr plating time. The nucleation density of copper was extremely high on the 2 s Cr-plated electrode, producing an extremely fine and uniform electrodeposit. However, on the 4 s Cr-plated electrode, the nucleation density of copper significantly reduced to one hundredth of that on the 2 s Cr-plated electrode, and then decreased slightly with increasing Cr plating time (thickness of Cr layer). These results appear to be associated with the *IR* drop across the Cr layer, including the surface Cr oxide/hydroxide film (termed the cathode film), which significantly reduces the driving force for the electrodeposition of copper under potentiostatic plating conditions.

1. Introduction

Copper electrodeposition from aqueous solution to form reliable, highly conductive current paths on printed circuit boards and associated devices is a widespread and important process in the electronics industry. Thin (12–70 μm thick) copper foils used in the printed circuit board industry are made by an electroforming process. Copper is electrodeposited on the substrate covered with a parting agent or release layer on which the quality of the thin copper foil largely depends.

Several researchers have reported on the utility of some materials, like organic agents, metals, and oxides, as release layers [1–4]. Among these materials, metals forming a uniform oxide film with high electronic conductivity on their surface are preferred for the substrates, because the thin copper foil should be detached easily from the release layer after electrodeposition. Thus, titanium, stainless steel and chromium have been preferred as substrates for the electroforming of copper foil because these metals and alloys form thin and uniform oxide films with all the properties required for the release layer on their surfaces.

As the electronic circuit density increases on printed circuit boards, the copper foil tends to be thinner (5–9 μm thick). Copper foil thinner than 9 μm is called ultra thin copper (UTC) foil. Production of UTC foil without pore like defects requires high nucleation density and uniform growth of copper in the electrodeposition process. It has been reported that the nucleation and growth of copper electrodeposits formed on oxide films of titanium and stainless steel are significantly influenced by the structure and properties of the films [3–7]. Delplanke et al. [3] reported that the copper nuclei density formed on an anodized film of titanium increased with increase in the pore density of the anodized film in which the pore acted as a copper nucleation site. Zhou and O'Keefe [5] also reported that the nucleus density of copper electrodeposits formed on an oxide film of stainless steel was highest and grew uniformly when the composition ratio of Cr/Fe in the film was lowest. Chromium is also very promising as a release layer for the UTC foil making process because it can be electrodeposited onto various substrates and its oxide film is easily formed in various environments and stable in copper electroplating solutions.

Although conventional chromium plating has a long history, its mechanism is not yet fully understood. However, it is generally accepted that a cathode film or a compound of chromium oxide and/or hydroxide [8–12] is formed at the interface of the chromium deposit and the electrolyte. For the UTC foil making process using the Cr release layer, copper is electrodeposited onto the cathode film of the Cr plating layer. Thus, the nucleation density of copper and its growth will be influenced by the surface structure and composition of the cathode film that is also determined by the electrochemical conditions applied to prior Cr plating.

The objectives of this work are to examine the influence of the prior Cr plating conditions on the nucleation and growth of copper formed on a Cr plated electrode, and then to evaluate the Cr plated layer as a release surface for the UTC foil.

2. Experimental details

A commercially pure copper sheet was used as a substrate for Cr electroplating. The surface of the copper sheet was polished with 1 μm diamond suspension, and then washed with distilled and deionized water before Cr plating. The electrolyte for the Cr plating was prepared with a concentration of 350 g L^{-1} of CrO_3 and 3.5 g L^{-1} of sulfuric acid, known as the 'Sargent Bath' [1, 8, 9]. The electrolyte for copper plating was prepared with a concentration of 1.0 M of $CuSO_4$ and 0.71 M H_2SO_4. The electrolytic cells for plating were set in a mantle with a temperature controller that allowed the electrolyte temperature to be maintained at a constant level of 30 °C for chromium deposition and 40 °C for copper deposition throughout the plating.

To examine the general deposition behavior of Cr from the prepared chromic acid electrolyte, a cathodic polarization test was performed at a scan rate of 2 mV s^{-1} using the conventional three electrode cell in which a saturated calomel reference electrode (SCE) and a platinum counter electrode were used. On the basis of the polarization curve, Cr was deposited on copper substrates for 15–60 s at 0.1–0.4 A cm^{-2}. The surface morphology and composition of the electrodeposits of Cr were observed using SEM and XPS (X-ray photoelectron spectroscopy) methods.

The potentiodynamic tests for deposition of copper from 1.0 M $CuSO_4$ and 0.71 M H_2SO_4 solution were performed to examine the effects of prior Cr plating time (or thickness of Cr layer) on the copper deposition behaviour. The tests were conducted at a scan rate of 0.5 mV s^{-1} using a conventional three electrode cell in which a SCE reference and a platinum counter electrode were used.

Copper was electrodeposited onto Cr-plated electrodes at −200 mV to examine the influences of prior Cr plating time on the nucleation and growth of the subsequent copper electrodeposits. The surface morphology of the copper electrodeposits formed on the Cr-plated electrodes was observed by SEM.

Electrochemical a.c. impedance spectroscopy (EIS) was used to measure the electrical resistance and capacitance of the Cr-plated electrodes in the copper plating solution (1.0 M of $CuSO_4$ and 0.71 M H_2SO_4) and in a dummy solution (1.0 M Na_2SO_4 + 0.71 M H_2SO_4). The frequency sweep was applied on a logarithmic scale (5 points per decade) from 10^5 Hz to 10^{-2} Hz using a superimposed sinusoidal signal of 5 mV r.m.s. at a Cu/Cu^{2+} equilibrium potential that is +93 mV vs SCE. The solutions were deaerated by purging with nitrogen gas throughout the tests. All the potentials in this work are referred to the SCE.

3. Results and discussion

3.1. *Chromium deposition*

A potentiodynamic polarization curve measured on the copper electrode in the chromic acid electrolyte (350 g L^{-1} CrO_3 + 3.5 g L^{-1} H_2SO_4) is shown in Figure 1. There are rising and falling features of current density in the potential region near −900 mV vs SCE. Some researchers have reported similar polarization behaviour in chromic acid electrolytes [9–13]. With cathodic polarization, the Cr^{6+} ions started to be reduced to Cr^{3+}, and a cathode film composed of chromium oxide and/or hydroxide begins to form at the interface between the Cr layer and electrolyte in the rising current region (about −800 mV). The depression in current after the maximum current occurred due primarily to the fact that the cathode film may act as a barrier for the Cr deposition [14, 15]. Metallic chromium was deposited from the electrolyte at potentials below that corresponding to the minimum current density (about −1100 mV).

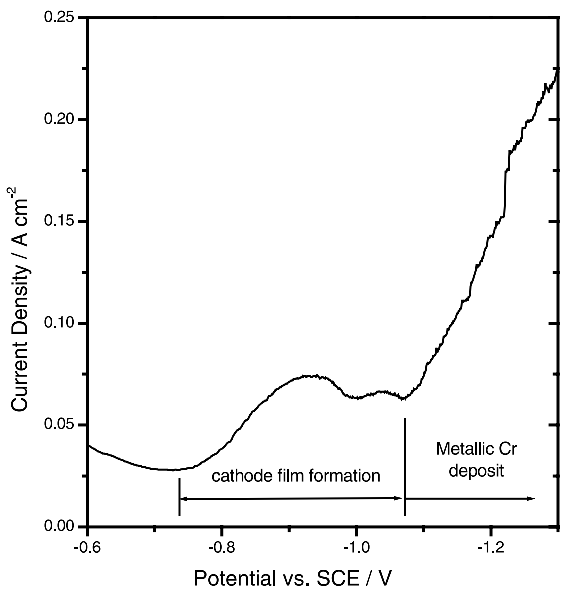

Fig. 1. Cathodic polarization curve of polished copper substrate measured at a scan rate of 2 mV s^{-1} in 350 g L^{-1} CrO_3 + 3.5 g L^{-1} H_2SO_4 solution at 30 °C.

The polarization curve in Figure 1 shows that the minimum current density for chromium deposition is 0.075 A cm^{-2} at about −1100 mV. The Cr deposit formed on the copper sheet from the chromic acid solution was observed using SEM. Figure 2 shows that the electrodeposits of Cr appear to be significantly different depending on the applied cathodic current density. At a low cathodic current density of 0.1 A cm^{-2}, a thin and flat layer of Cr was formed, and then granular Cr particles were formed on the thin and flat electrodeposited layer at a higher cathodic current density of 0.2 A cm^{-2} (Figure 2(b)). The nucleation density of Cr particles formed on the thin and flat Cr layer increased with increase in the cathodic current density, due primarily to the higher cathodic overpotential at the higher cathodic current density (Figure 2(c)). The thin and flat layer formed at the initial stage of electrodeposition was confirmed to be Cr by EDX analysis, as shown in Figure 2(d).

Since the aim of this study is to investigate the nucleation and growth process of copper on the Cr-plated layer for the UTC foil making process, the granular particles of chromium would be harmful to the production of a thin, uniform and pore free copper foil by electroforming. Thus, the cathodic current density of 0.1 A cm^{-2}, at which only the thin and flat Cr layer is formed, was employed in all the subsequent copper plating.

3.2. *Copper deposition on Cr layer*

Cathodic polarization tests were performed on Cr plated electrodes in the acidic copper sulfate electrolyte, and the results are presented in Figure 3, in which the arrow (a) indicates the standard potential of the Cu^{2+}/Cu^0 redox couple (+93 mV vs SCE) [6]. The potential for electrodeposition of copper on the Cu sheet without a chromium layer appears at the most positive potential region. The potential for electrodeposition of copper on the Cr-deposited layer, however, becomes more negative with increased prior Cr deposition time (or Cr layer thickness). This result demonstrates that the thicker the chromium layer, the greater overpotential is required for the nucleation and growth of copper. The deposition potential region shown in Figure 3 is similar to the overpotential region (< 200 mV) for copper deposition observed by other researchers on variously treated Ti surfaces and on oxidized stainless steels [3–7]. The polarization curve for the electrode without a chromium layer shows higher current density in the potential region above −30 mV, but in the more negative potential region it becomes lower than those for chromium deposited electrodes. The copper deposit formed on the electrode without a chromium layer shows a smoother surface than those on other chromium plated electrodes after polarization. Thus, the reason for the lower current density of the copper electrodes without a chromium

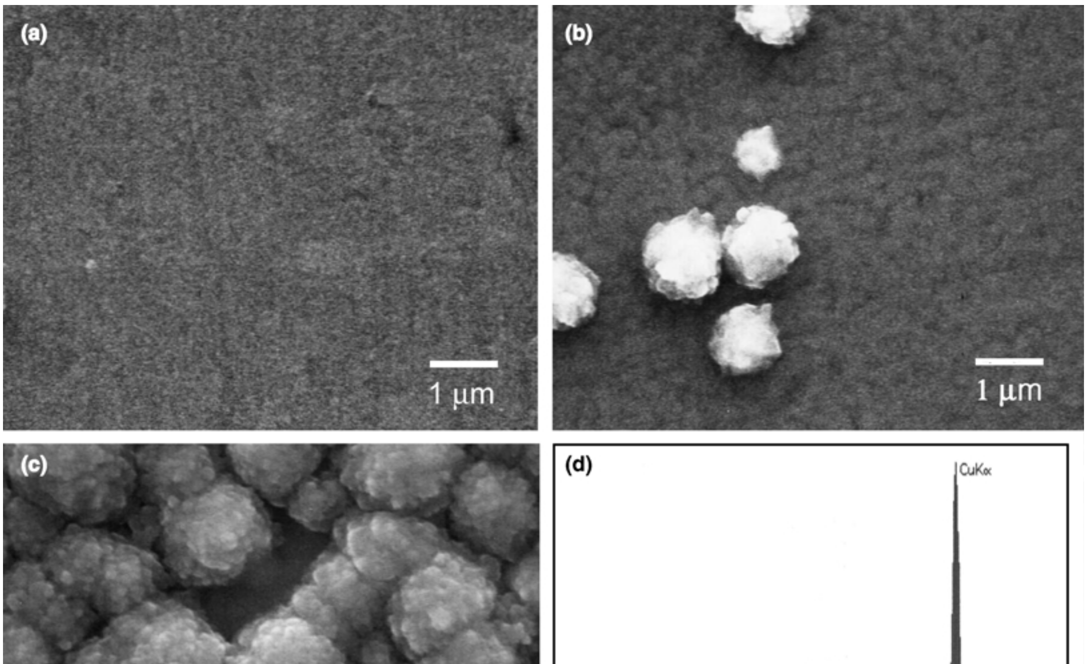

Fig. 2. SEM micrographs of Cr electrodeposited on polished copper substrates (a) for 30 s at 0.1 A cm^{-2}, (b) for 30 s at 0.2 A cm^{-2}, (c) for 30 s at 0.4 A cm^{-2} in 350 g L^{-1} CrO_3 + 3.5 g L^{-1} H_2SO_4 solution at 30 °C, and (d) is EDX spectrum on flat surface region of specimen.

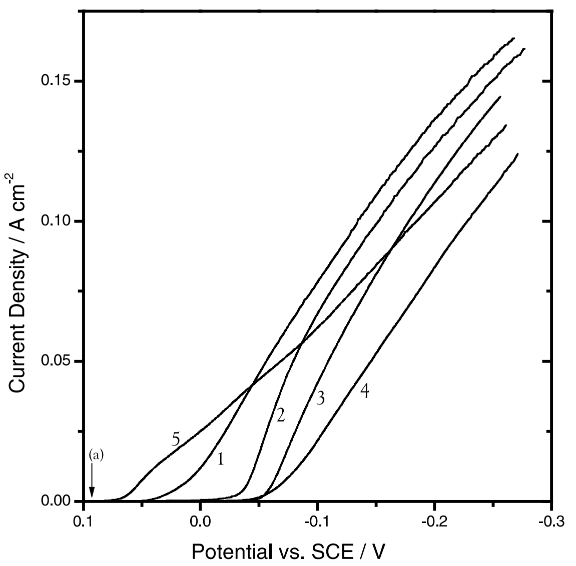

Fig. 3. Effects of Cr plating time on the cathodic polarization response of Cu on Cr layer in 1.0 M $CuSO_4$ + 0.71 M H_2SO_4 solution at 40 °C. Cr layers were electrodeposited on polished copper substrates for 0, 2, 8, 30, 60 s at a current density of -0.1 A cm^{-2} in 350 g L^{-1} CrO_3 + 3.5 g L^{-1} H_2SO_4 solution, at 30 °C. Cr deposition time: (1) 2 s, (2) 8 s, (3) 30 s, (4) 60 s, (5) no Cr deposit.

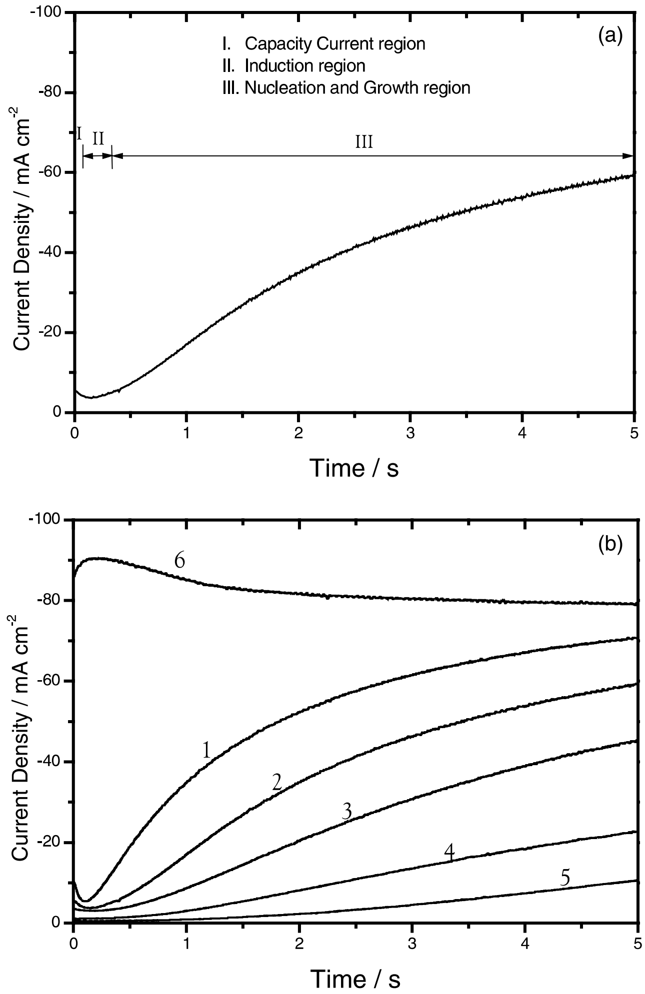

Fig. 4. Current–time transients for Cu electrodeposition on Cr layer/Cu at -200 mV vs SCE in 1.0 M $CuSO_4$ + 0.71 M H_2SO_4, 40 °C solution. (a) Typical current transient obtained for the nucleation and growth of copper from a pure copper sulfate electrolyte on Cr-deposited electrode. (b) Prior to Cu electrodeposition, the Cr were electrodeposited on polished copper substrate for 2, 4, 15, 30 and 60 s at -0.1 A cm^{-2} in 350 g L^{-1} CrO_3 + 3.5 g L^{-1} H_2SO_4 solution at 30 °C. Cr deposition time: (1) 2 s, (2) 4 s, (3) 15 s, (4) 30 s, (5) 60 s, (6) no Cr deposit.

layer seems to be that the growth mode is two dimensional, while the others have a three dimensional dendrite structure that has a much larger true area than a flat surface.

A typical current transient curve recorded when a cathodic potential was applied to a chromium plated electrode is shown in Figure 4(a). The current transient curve can be divided into three periods [7]; capacitive current period, induction period and nucleation and growth period. The capacitive current period was defined as that for charging a double layer on an electrode, and happened in 50 ms or shorter on various titanium electrodes. Generally, the time to charge the double layer depends on the applied potential and its capacitance.

Figure 4(b) shows current–time transients for deposition of copper at -200 mV on the electrodes plated with Cr for various times. The current densities show a minimum value for a short time, and thereafter increase with time. On electrodes plated with Cr for a longer time than 15 s, the current transients did not show the minimum value (curves 3, 4 and 5 in Figure 4(b)) due presumably to the capacitive nature of chromium deposits as will be discussed later.

The induction period for electrochemical nucleation shown in Figure 4(a) appears to be associated with the time required for the formation of new stable nuclei. It was reported [16] that the induction period is that during which some clusters under the critical size develop and disappear repeatedly until a nucleus with a critical size has formed. This depends on the overpotential applied to the electrode. Figure 4(b) shows that the longer the prior chromium plating time, the longer the induction period, implying that the thicker Cr layer, including the cathode film, may reduce the overpotential for the electrodeposition of copper. On electrodes plated with Cr under the same conditions, the induction period becomes longer with decreasing cathodic potential or cathodic overpotential as shown in Figure 5. These results suggest that as the electrodeposit layer of Cr grows thicker, the actual cathodic overpotential for the electrodeposition of copper decreases at the same applied potential.

Figure 6 shows that the cathodic current density in the initial nucleation and growth period of the current transient curves in Figure 4, after passing the capacitive current and induction period (t_0), is linear with $(t-t_0)^{3/2}$, which corresponds to the progressive nucleation model under diffusion controlled three-dimensional growth. According to this model, the cathodic current density under potentiostatic electrodeposition is proportional to $t^{3/2}$ (t is the nucleation time). For the instantaneous

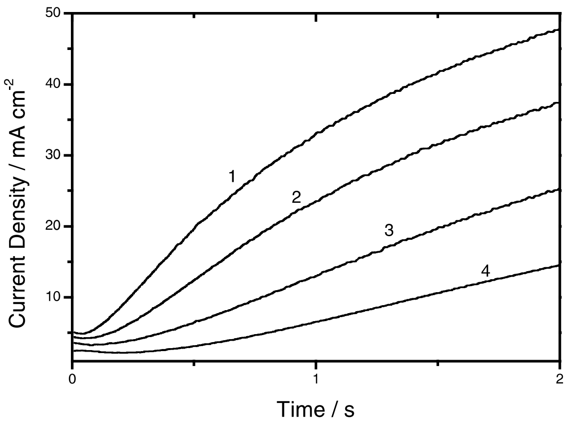

Fig. 5. Effect of applied potential on the potentiostatic current transient of Cu on the electrodeposited Cr layer/Cu in 1.0 M $CuSO_4$ + 0.71 M H_2SO_4, 40 °C solution. Prior to Cu electrodeposition on Cr, the Cr layers were electrodeposited on polished copper substrate for 4 s at −0.1 A cm^{-2} in 350 g L^{-1} CrO_3 + 3.5 g L^{-1} H_2SO_4 solution, at 30 °C. Applied potential: (1) −240, (2) −220, (3) −200 and (4) −180 mV vs SCE.

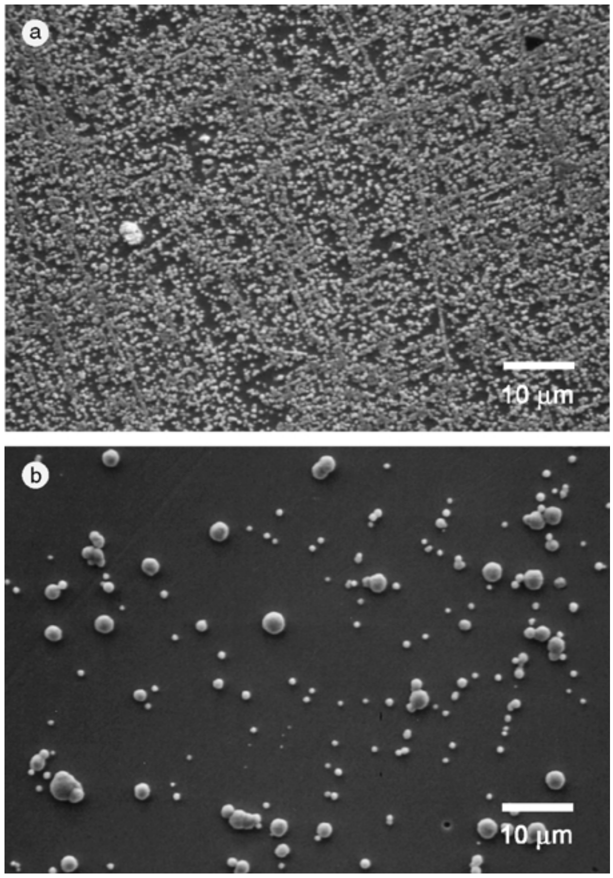

Fig. 7. SEM micrographs showing the influence of prior Cr electrodeposition on Cu nuclei electrodeposited for 5 s on Cr layer/Cu at −200 mV vs SCE in 40 °C, 1.0 M $CuSO_4$ + 0.71 M H_2SO_4 solution. Cr layers were electrodeposited on polished Cu substrate for (a) 2 s and (b) 4 s at −0.1 A cm^{-2} in 30 °C, 350 g L^{-1} CrO_3 + 3.5 g L^{-1} H_2SO_4 solution.

nucleation model, however, under the diffusion controlled three-dimensional growth, the cathodic current density is proportional to $t^{1/2}$ [17].

It is evident in Figure 6 that, as the Cr plated layer becomes thicker, the time during which progressive nucleation of copper is dominant increases; on a 2 s chromium plated electrode, progressive nucleation occurred only up to the initial 0.6 s of copper deposition, while it occurred to over 5 s on the 60 s Cr-plated electrode. A progressive 3D nucleation mechanism can be effective in an electrodeposition process where the diffusion zone of each nucleus does not overlap. Markov et al. [18] suggested that the size exclusion zone for nucleation is much larger than the nucleus size. The SEM micrograph of Figure 7(a) shows that the nuclei of copper formed on the 2 s Cr-plated electrode are so fine and large in number that there is not enough space to

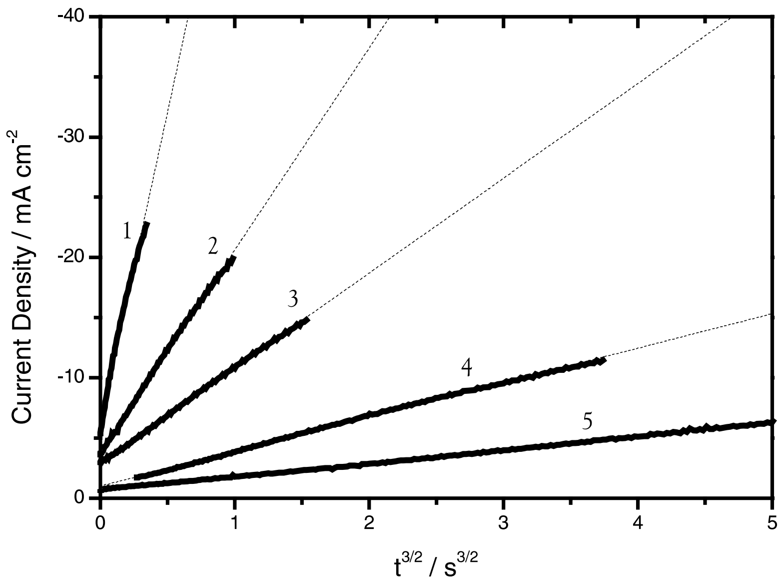

Fig. 6. Current density against $t^{3/2}$ for potentiostatic currents transients of Cu electrodeposition on Cr layers/Cu based on the data in Figure 4. Cr deposition time: (1) 2 s, (2) 4 s, (3) 15 s, (4) 30 s, (5) 60 s.

nucleate between nearer neighbours. Further, most of the nuclei may be nucleated almost simultaneously, as confirmed by their similar size. This means that the progressive nucleation process ends in the very early stages of deposition, as confirmed in Figure 6. However, for the 4 s Cr-plated electrode, there is a large distance between copper nuclei of diverse sizes, confirming that the nucleation occurs at different times, thus suggesting progressive nucleation.

After the progressive nucleation, a current transient for the electrodeposition of copper follows the diffusion controlled 3D instantaneous nucleation model in which the current density is linear with $t^{1/2}$, as shown in Figure 8. In this case, diffusion zones of nuclei overlap. Figure 8 shows that the time to reach the instantaneous nucleation relation gets longer with increased Cr plating time.

Figure 9 shows the copper nucleation density on the Cr plated electrodes as a function of prior Cr deposition time. There is evidently a marked dependence of copper nucleation density on the Cr plating time; the copper nuclei density decreases dramatically with increasing from 2 to 8 s, and then gradually after 8 s.

3.3. *XPS depth profile of chromium deposits*

Figure 10 shows XPS composition depth profiles of the Cr layers formed on copper sheet. For chemical analysis by XPS, all the specimens were sputtered at the same time in the same chamber, and analysed in sequence. During sputtering, the current density was maintained at 0.035 μA mm^{-2} [15].

All the specimens analysed have a similar depth profile from the surface to 4.5 min sputtering, but the

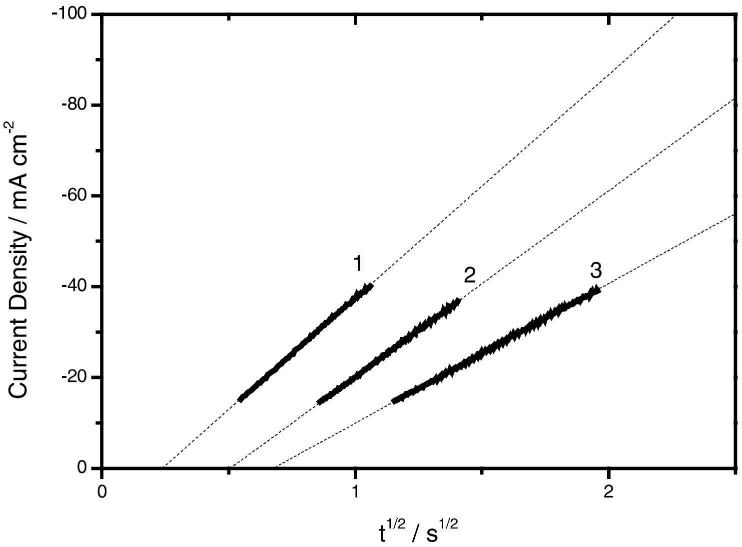

Fig. 8. Current density against $t^{1/2}$ for potentiostatic currents transients of Cu electrodeposition on Cr layers/Cu based on the data in Figure 4. Cr deposition time: (1) 2 s, (2) 4 s, (3) 15 s.

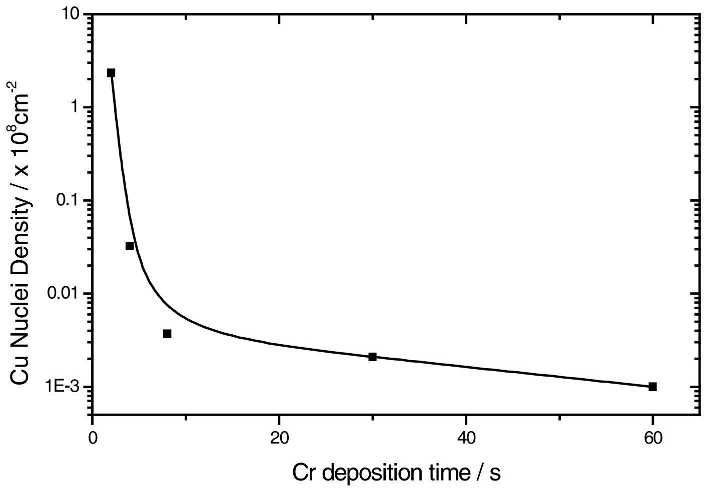

Fig. 9. Influence of prior Cr deposition time on Cu nuclei electrodeposited for 5 s on Cr layer/Cu at −200 mV vs SCE in 40 °C, 1.0 M Cu SO_4 + 0.71 M H_2SO_4 solution. Cr layers were electrodeposited on polished Cu substrate for (2–60) s at −0.1 A cm^{-2} in 30 °C, 350 g L^{-1} CrO_3 + 3.5 g L^{-1} H_2SO_4 solution.

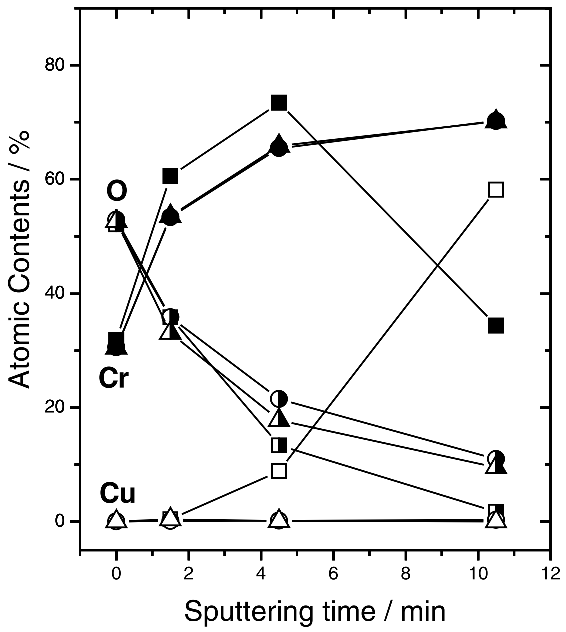

Fig. 10. XPS composition profiles in depth for Cr electrodeposits formed for (2, 8 and 30 s) at -0.1 A cm^{-2} in 30 °C, 350 g L^{-1} CrO_3 + 3.5 g L^{-1} H_2SO_4 solution. Elements: (solid) Cr, (half solid) O, (open) Cu concentration; Cr deposition time: (square) 2 s, (circle) 8 s, (triangle) 30 s.

specimen plated for 2 s with Cr shows a different profile, that is, the Cr concentration is slightly higher after 1.5 and 4.5 min of sputtering. In contrast, the oxygen concentration of the specimen is somewhat lower than that of other specimens after 4.5 min of sputtering.

Other important features shown in Figure 10 are the oxygen and Cr profiles of the Cr layers deposited for 8 and 30 s. They behave similarly during the initial 10.5 min of sputtering. This suggests that the oxygen rich region of the surface is a cathode film that is formed externally during Cr plating [14]. The cathode film can be divided into two parts; the L-film, located on the electrolyte side of the film and soluble in electrolyte or acidic solution, and the C-film, located on the electrode side and is not easily dissolved in electrolytes [15]. It was also reported that once the C-film is established, it does not change thickness and composition during plating. Accordingly, the C-film has been formed in the initial 8 s of Cr plating, and the C-films formed for 2 s are not complete. Mandich reported that the cathode film is composed of chrome oxide complex, and that the L-film is composed of an olated chromium complex. The C-film is more polymerized than the L-film [19, 20]. It seems that the C-film formed in less than 8 s is less dense, and has a lower degree of polymerization than that formed over 8 s or longer. These structural and composition differences in the C-film, which are sensitive to the prior Cr plating time, may produce large differences in the nucleation density of copper formed on electrodes plated with Cr, as shown in Figures 7 and 9.

3.4. *AC impedance spectra*

An ac impedance method was introduced to examine the copper nucleation behaviour on the electrodes plated with Cr. The impedance of the Cr plated electrodes was measured in a dummy electrolyte (1.0 M Na_2SO_4 + 0.71 M H_2SO_4) in which cupric ions in the acidic $CuSO_4$ solution were replaced with sodium ions.

Figure 11 shows the influences of Cr plating time on the Nyquist plot of the Cr plated electrodes measured at +90 mV in the dummy solution. As the chromium plating time increases, the impedance loop gets larger, and the second loop in the low frequency region was somewhat distorted. For simplification, the basic equivalent circuit model described in Figure 12(a) was applied

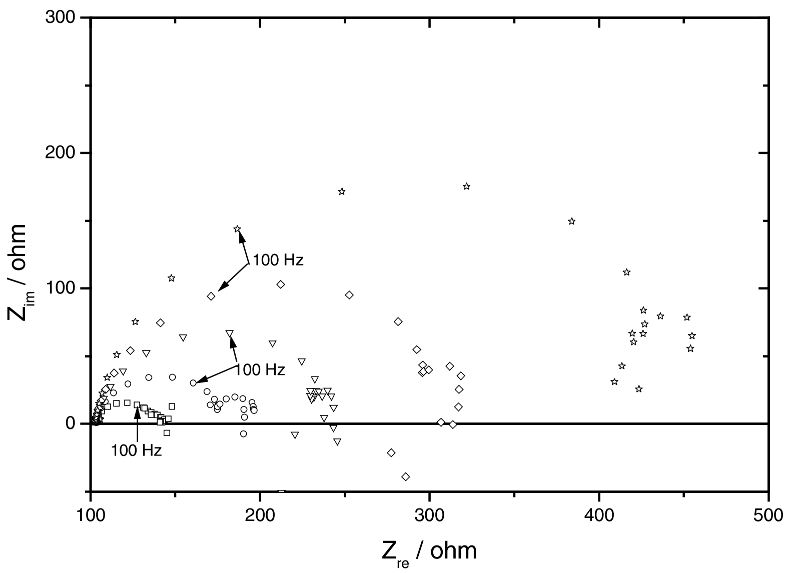

Fig. 11. Nyquist plot of Cr deposits formed for (2–60) s at -0.1 A cm^{-2} in 30 °C, 350 g L^{-1} CrO_3 + 3.5 g L^{-1} H_2SO_4 solution. Impedance tests were performed at +90 mV vs SCE in 40 °C, 1 M Na_2SO_4 + 0.71 M H_2SO_4 solution. Cr deposition time: (□) 2, (○) 4, (▽) 15, (◇) 30 and (★) 60 s.

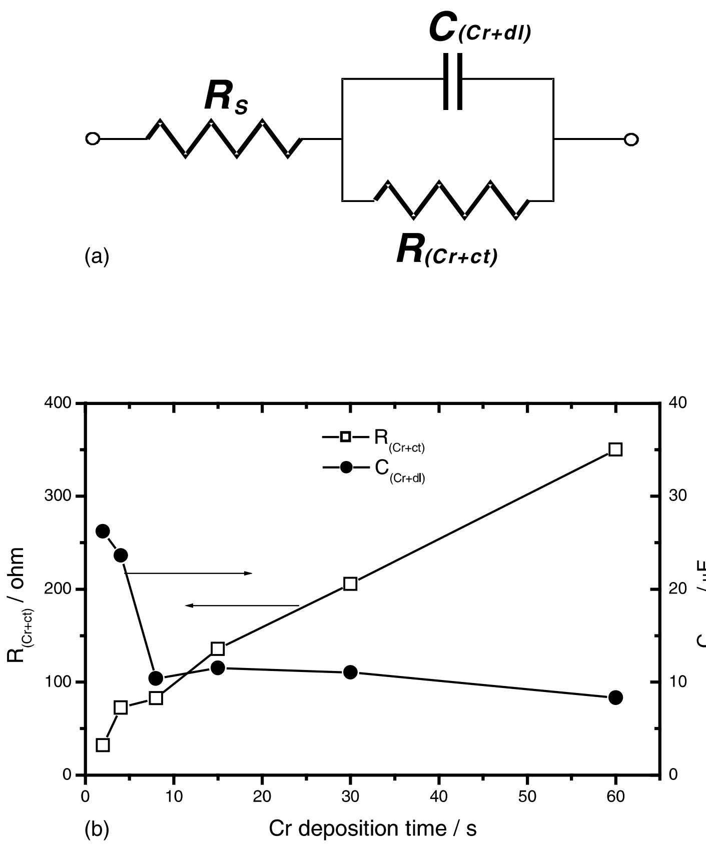

Fig. 12. Equivalent circuit (a) used to simulate the high frequency region of impedance data of Figure 11, and (b) the resistance and capacitance of Cr deposit layers as a function of Cr deposition time.

to the impedance loops acquired in the high frequency region. Figure 12(b) shows the capacitance and resistance as a function of the chromium deposition time. It is noted that the resistance of the Cr layer increased appreciably in the initial 4 s and afterwards gradually. In contrast, the capacitance of the Cr layer shows a sharp drop in the initial 8 s and thereafter remains almost constant at 10 μF. The sharp drop in the capacitance in the initial 8 s appears to be associated with the formation of C-film [11, 12]. The small change in the capacitance after the 8 s Cr plating suggests that the C-film remained stable after its formation. Nielson et al. studied the texture of Cr electrodeposits formed using d.c. current, and found that some nano particles of Cr_2O_3 were codeposited with chromium metal in the plating processes [19]. Thus, the gradual increase in the resistance of the chromium layer (Figure 11(b)) after the initial 8 s of Cr plating appears to be associated with the Cr_2O_3 'nano' particles codeposited in metallic chromium.

3.5. *Models for copper nucleation and growth on chromium electrodeposits*

A question is addressed why nucleation density of copper electrodeposit formed on the Cr plated electrodes is so sensitive to the prior Cr plating time (or Cr layer thickness) as shown in Figures 7 and 9. It is significant that there are similarities between the current transient curves 1 to 4 in Figure 4 and those in Figure 5. The effects of reduction in the applied cathodic potential or increase in cathodic overpotential is parallel to the effects of increase in the Cr plating time, on the current transient curve for the electrodeposition of copper. In other words, the increase in the Cr plating time (or the thickness of Cr layer) appears to reduce the cathodic overpotential for the electrodeposition of copper. It was reported that formation of a cathode film induced an *IR* drop at the surface of an electrode and hence reduced the potential difference of electrolyte–electrode interface or the electrode potential [12]. Electrodeposited Cr has a higher electrical resistance than metallic Cr due to the high defect density and 'nano' chromium oxide particles dispersed in the Cr electrodeposit [21]. Therefore, for a potentiostatic electrodeposition of Cr, the cathode film and thicker Cr layer induce a large *IR* drop, reducing the cathodic overpotential for the subsequent electrodeposition of copper, as shown in Figure 13. At the reduced electrode potential or at the reduced cathodic overpotential, the driving force for the copper nucleation will be low and would be resulted in low nucleation density of copper. Figure 13, shows how *IR* drop occurs across the Cr plated layer including the cathode film and hence acts as a barrier to the copper deposition process.

The composition and/or structure of the cathode film may also affect nucleus density of copper. The XPS composition profiles in Figure 10 clearly show that the

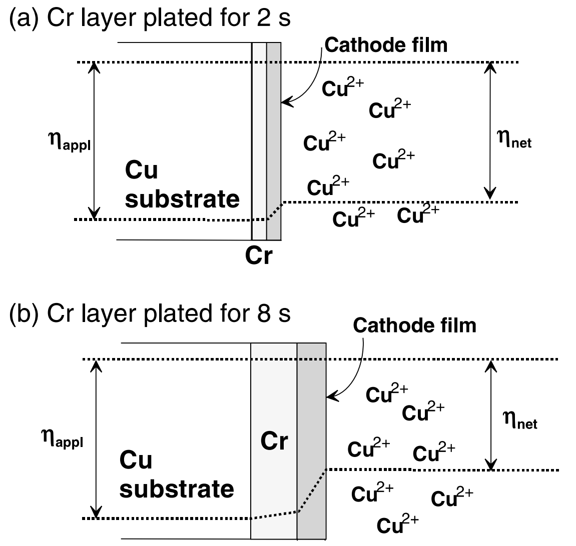

Fig. 13. Schematic diagram showing the effects of *IR*-drop developed across the Cr layer on the cathodic overvoltage for Cu electrodeposition in acidic copper sulfate electrolyte, (a) 2 s Cr-plated electrode, (b) 8 s Cr-plated electrode in 350 g L^{-1} CrO_3 + 3.5 g L^{-1} H_2SO_4 solution; η_{appl} is applied overvoltage, η_{net} is net overvoltage.

electrode plated with Cr for 2 s contains higher Cr concentration and lower oxygen concentration profile in the outer layer or C-film compared with those for others. Thus, it can be proposed that the cathode film formed for 2 s has a lower Cr oxide density and a lower degree of polymerization than that formed for longer plating time. Thus, the cathode film formed on the 2 s Cr-plated layer may make it easy for electrons to pass through for the subsequent plating of copper. This may lead to higher nucleation density of copper on the 2 s Cr-plated electrode compared with that on the other electrodes under the same electrodeposition conditions.

4. Conclusions

The following conclusions were drawn:

(i) The surface morphology of Cr electrodeposited on copper sheet depended on the applied cathodic current density. At a low current density such as 0.1 A cm^{-2}, a thin and flat layer of Cr was formed without granule type deposits. On the other hand, at 0.2 A cm^{-2} or higher, Cr particles with a granule type were formed on the thin and flat Cr layer.

(ii) The typical current transient curve for electrodeposition of copper is divided into three regions; capacitive current region, induction region, and nucleation and growth region. The induction time for the nucleation of copper formed on the Cr-plated electrode, defined as the period from the end of charging double layer to a new nucleus being formed, increased either with decreasing cathodic overpotential or with increasing Cr plating time.

(iii) Copper electrodeposited on the Cr-plated electrode was initially nucleated and grew according to a three-dimensional diffusion controlled progressive nucleation process, and later according to an instantaneous nucleation process. The period during which copper nucleation is controlled by the diffusion controlled progressive nucleation process decreases with increasing Cr plating time.

(iv) The nucleation density of copper formed on Cr-plated electrodes is a function of prior Cr plating time; it decreases with increasing Cr plating time. This is due primarily to the *IR*-drop across the Cr-plated layer including the cathode film, which reduces the driving force for the electrodeposition of copper.

Acknowledgements

The authors thank the Ministry of Commerce, Industry and Energy of the Republic of Korea and IlJin Copper Foil Co., for the financial support. This study was also partially supported by Brain Korea (BK21) project.

References

1. C.B. Yates and A.M. Wolski, *US Patent 3 998 601* (1976).
2. G.M. Rao and W.C. Cooper, *Hydrometall.* **4** (1979) 185.
3. J.L. Delplancke, M. Sun, T.J. O'Keefe and R. Winand, *Hydrometall.* **23** (1989) 47.
4. K.S. Teng, PhD dissertation, University of Missouri-Rolla (1995).
5. Z. Zhou and T.J. O'Keefe, *J. Appl. Electrochem.* **28** (1998) 461.
6. J.L. Delplancke, M. Sun, T.J. O'Keefe and R. Winand, *Hydrometall.* **24** (1990) 179.
7. H. Sun, J.L. Delplancke, R. Winand and T.J. O'Keefe, Copper 91 – Cobre 91 Vol. III (1991), p. 405.
8. J.P. Hoare, *J. Electrochem. Soc.* **126** (1979) 190.
9. J.P. Hoare, *Plat. Surf. Finish.* **76**(9) (1989) 46.
10. J.S. Kim, PhD dissertation, Korea Advanced Institute of Science and Technology (1998), p. 134.
11. C. Fabricius and G. Sundholm, *J. Appl. Electrochem.* **14** (1984) 797.
12. J. Pang, A. Briceno and S. Chander, *J. Electrochem. Soc.* **137** (1990) 3447.
13. J.L. Fang, N-J. Wu and Z.-W. Wang, *J. Appl. Electrochem.* **23** (1993) 495.
14. K. Yoshida, A. Suzuki, K. Doi and K. Arai, *Kinzoku Hyomen Gijutsu* **30**(7) (1979) 338.
15. K. Yoshida, Y. Tsukahara and K. Koyama, *Kinzoku Hyomen Gijutsu* **30**(9) (1979) 457.
16. G. Gunawardena, G. Hills, I. Montenegro and B. Scharifker, *J. Electroanal. Chem.* **138** (1982) 225.
17. H.R. Thirsk and J.A. Harrison, 'A Guide to the Study of Electrode Kinetics' (Academic Press, New York, 1972), p. 115.
18. I. Markov, A. Boynov and S. Toschev, *Electrochim. Acta* **18** (1973) 377.
19. N.V. Mandich, *Plat. Surf. Finish.* **84**(5) (1997) 108.
20. N.V. Mandich, *Plat. Surf. Finish.* **84**(6) (1997) 97.
21. P. Leisner, G. Bech-Nielsen and P. Moller, *J. Appl. Electrochem.* **23** (1993) 1232.